

PROPERTIES OF INDIVIDUAL X-RAY SOURCES

(Invited Discourse)

LAURENCE E. PETERSON*

Dept. of Physics, Space Physics Group, University of California, San Diego, La Jolla, Calif., U.S.A.

Abstract. Observations to determine the spectra and time variations of hard X-rays from cosmic sources have been made from balloons and from the OSO-III satellite. These data have been obtained using actively collimated scintillation counters with apertures between 6 and 24° FWHM, areas between 10 and 50 cm² and which operate over the 10–300 keV range. The Crab Nebula has been observed on three occasions over a 22-month period between September 1965 and July 1967. The power law spectrum has a number index of 2.0 ± 0.1 . No long-term changes were observed over the 30–100 keV range with a limit at 3%/yr. A balloon search with a 10 cm² Ge(Li) detector for X-ray lines at 62.5 keV, 110 keV and 180 keV due to heavy element radioactive decays which would be produced in the initial Crab explosion based on the Cf²⁵⁴ hypothesis has resulted in upper limits at about 10^{-3} γ -rays cm²-sec. This is about a factor of 20 above the predicted levels. Simultaneous X-ray and optical observations of SCO XR-1 from OSO-III confirm that X-ray and optical flaring are indeed coincident phenomena, and that although the X-ray intensity increases about a factor of two during the flare, the equivalent temperature of the excess radiation is nearly the same as that of the quiescent object. Upper limits, 95% confidence, on the flux of M-87 at 40 keV have been obtained. These are inconsistent with the flux of 1.2×10^{-4} photons/cm²-sec-keV reported in the literature. CYG X-1 has been observed to have a power law of number index 2.0 ± 0.2 . The OSO-III has observed a number of sources in the southern skies including NOR XR-2 and the variable source Centaurus XR-2.

1. Introduction

In this paper, significant previous results are reviewed and some new data presented which have been obtained relative to point X-ray sources by the UCSD Gamma-Ray Astronomy Group. Most of the observations obtained since 1965 from balloons have been concerned with the spectra and time variations of these sources in the northern skies. These observations have been primarily made with scintillation counters and cover 15–300 keV energy range. Although most of the earlier data were obtained with instrumentation flown from high altitude balloons, recent observations have been obtained with the OSO-III satellite, which was launched March 8, 1967, and from which preliminary results are now available.

2. Instrumentation

Detector systems which have been developed at UCSD for these observations over the past five years are based upon the principle of the actively shielded collimated scintillation counter. Use of these detectors was started in a collaboration with Ken Frost (Frost *et al.*, 1966) of the Goddard Space Flight Center in 1962, and many preliminary data necessary to determine background properties of the detector in its radiation environment were obtained in a series of experiments on the OSO-I satellite

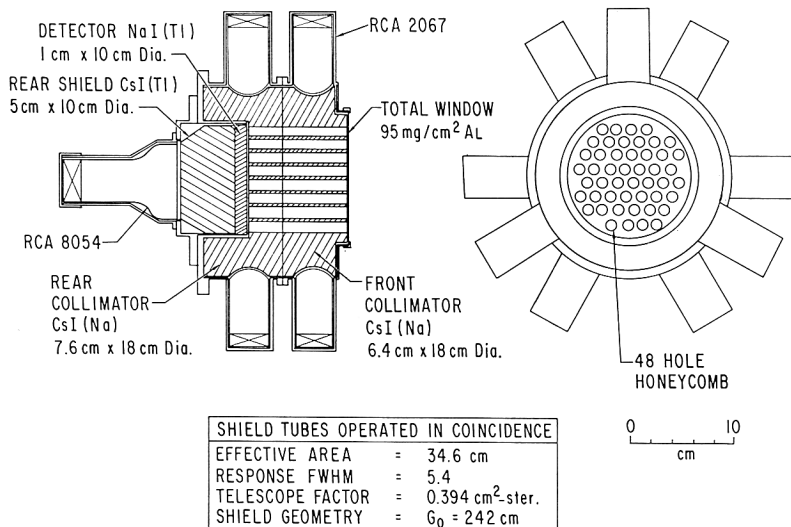
* Other members of the UCSD Gamma-Ray Astronomy Group who have contributed to this work include H. S. Hudson, A. S. Jacobson, J. L. Matteson, D. McKenzie, R. M. Pelling, and D. A. Schwartz.

(Peterson, 1966) and at balloon altitudes. The detector flown on the OSO-III satellite, which resulted from these early studies, has been described in the literature (Hicks *et al.*, 1965). This 10 cm² detector with a 23° full width half maximum response (FWHM) was identical to the detector which was used during many of the early balloon observations (Peterson and Jacobson, 1966).

The design criterion for these detectors is to construct a collimating shield around the photon sensing element so that the total radiation through the front aperture, which consists of atmospheric X-rays secondary to cosmic rays and cosmic X-rays due to the diffuse sky component, is approximately equal to the remaining, or 'true detector background' consisting of effects due to shield leakage, Compton scattering in the shield, neutron interactions in the central detector, and possibly other interactions which are not presently understood. The most successful way to build a detector with such a property at small solid angles Ω is to design the shield of scintillation material, such as CsI(Na). This is observed by a photomultiplier, which is connected in electrical anticoincidence with a central scintillation counter, usually of NaI(Tl). The shield thickness is optimized according to the relation

$$\frac{\Omega}{4\pi} \cong e^{-\bar{t}/\tau},$$

where \bar{t} is the average thickness of the shield and τ is the photon mean free path in the shield material at the highest energy where operation is desired. Although more background rejection may be obtained by constructing a shield which is thicker, for a given



ACTIVE HONEYCOMB DETECTOR - MOD 2
15 - 500 KeV

Fig. 1. An actively collimated hard X-ray detector developed recently at UCSD. The aperture is formed by a honeycomb hole pattern. Cosmic-ray produced background and higher energy γ -ray events are rejected by anticoincidence circuitry.

aperture the signal-to-noise will be increased by only a factor of $\sqrt{2}$ at a considerable expense in weight, deadtime and cost. Detectors vary from the simple cylindrical geometry designed for the OSO-III to a model which uses a CsI collimator consisting of holes drilled in a honey-comb pattern and a separate 'well' to provide side and rear shielding. This 48 cm² detector with a 8.4° FWHM operative detector and its properties have also been described in the literature (Peterson *et al.*, 1968).

The latest version developed at UCSD by J. L. Matteson and R. M. Pelling and shown in Figure 1 has 36 cm² area and an aperture of 5.4° FWHM. This detector, which has no inert mass inside the shield, uses a NaI(Tl)/CsI(Tl) 'phoswich' to provide attenuation from the rear. The honeycomb collimator of CsI(Na) is observed with a large number of phototubes in coincidence in order to detect the lowest energy photons scattered into the shield and therefore to improve the background rejection.

Detectors such as these, before being placed in operation, are test flown on a balloon at the altitude where the observations will be eventually made in order to determine the background properties in the correct radiation environment. The background at 3 gm/cm² over Palestine, Texas, is also very similar to that encountered in an OSO satellite at 550 km, 33° inclination. The test gondola contains an additional scintillation counter which may be moved in front of the aperture and connected in anticoincidence. Spectra of the central detector are obtained with the aperture

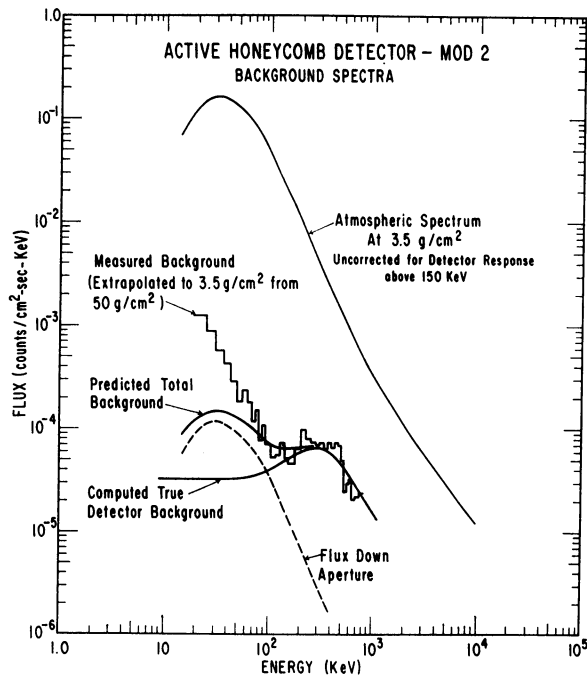


Fig. 2. The aperture and background properties of the detector shown in Figure 1 at balloon altitudes. The isotropic background spectrum is attenuated by the aperture solid angle factor of 1000 and is added onto various leakage and scattering contributions in the detector due to its total radiation environment.

blocked and unblocked, with the anticoincidence turned on and off and with the shield operating in different modes in order to determine various contributions to the background. Figure 2 shows typical test data obtained on the detector shown in Figure 1.

The upper curve indicates the total atmospheric spectrum measured at 3 gm/cm^2 (Peterson *et al.*, 1967). At this altitude the total atmospheric plus diffuse cosmic spectrum forms nearly an isotropic distribution. If the detector shield were perfect, the measured flux through the aperture would therefore be the atmospheric background reduced by the ratio of $\Omega/4\pi$, as indicated by the dotted line. Background not due to external fluxes entering the aperture, which is determined with the collimator blocked, is due mostly to Compton scattering of higher energy γ -rays which leak through the finite shield thickness and scatter in the central detector. A Monte-Carlo computer program for determining this effect has been developed by J. L. Matteson. Using the known atmospheric spectrum, this model technique predicts a true detector background which is indicated by the solid line. The sum of this background plus the flux through the aperture should equal the total background spectrum measured with the aperture opened, assuming no cosmic point sources are within the aperture.

The measured spectrum is shown in the histogram and agrees very well with the predictions at energies above about 80 keV. At the lower energies, however, an effect which is not directly predicted from the interactions of radiation with matter produces an additional exponential background spectrum extending to the lowest energies. This effect is apparently caused by large noise pulses produced by phosphorescent effects in the phototube, photocathode, or the scintillation material (Jerde *et al.*, 1967), and may be reduced by eliminating fast decay events in the central detector. We feel that the background properties of these detectors are sufficiently well understood so that similar systems of much larger area and smaller aperture could be designed and that these techniques could be extended to higher energies.

In order to make observations of cosmic sources from a balloon, a system is required which provides pointing and data transmission (Peterson *et al.*, 1967) facilities. One of the more recent balloon gondolas flown at UCSD is shown in Figure 3. This consists of a bottom structure or base which is suspended through a rigging mechanism and the parachute to the balloon. A large yoke containing an equatorial axis is free to move in azimuth about a vertical axis. This axis is driven in azimuth by a servo which obtains error signals either from a magnetometer system or from a star tracker and aligns the equatorial axis in the N-S meridian plane. This axis is also driven in elevation by a servo which also obtains error signals from the star tracker, or may be operated from ground command, based on the known latitude of the balloon. The detector may be controlled to a number of preselected declination and hour angle positions with reference to the equatorial axis. A command system permits tracking mode selection, real-time star search and acquisition, and dec/h.a. selection.

In practice the device is usually operated in a drift scan mode, in which a detector is fixed at the appropriate declination corresponding to the source and at some angle about the polar axis. As the earth rotates, the source then drifts through the aperture

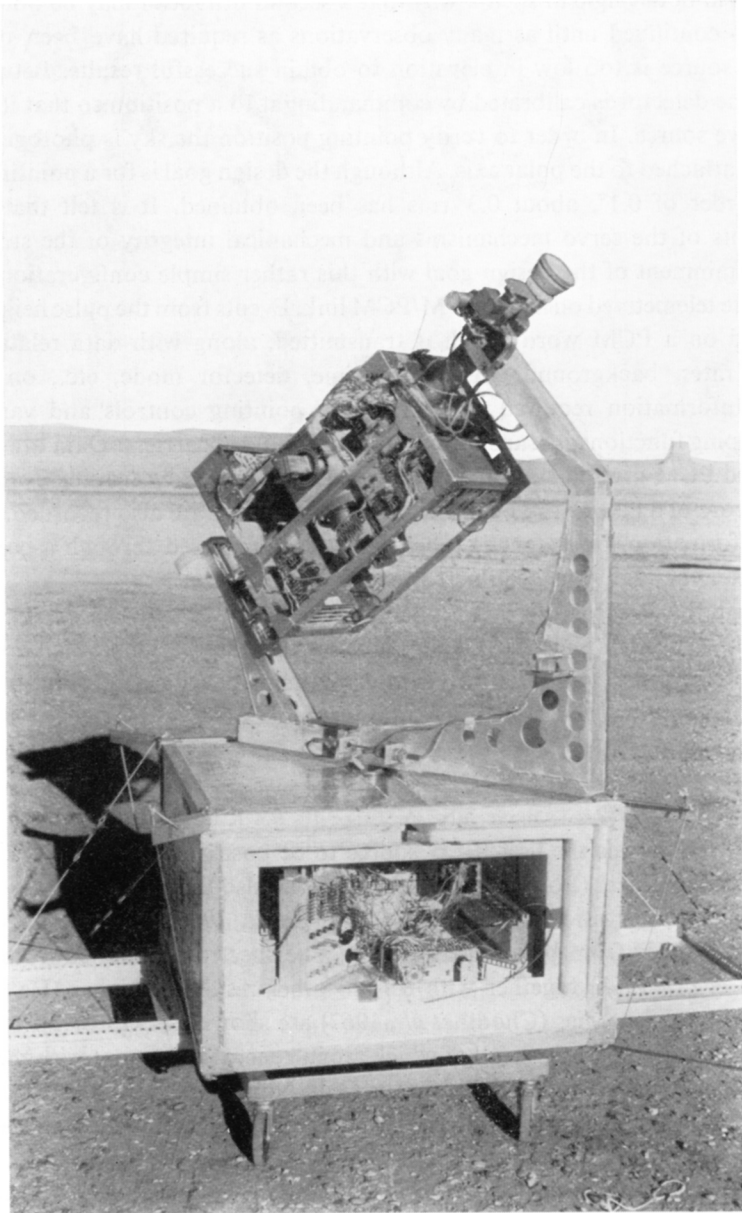


Fig. 3. The equatorial axis gondola used to orient detectors similar to that shown in Figure 1. The bottom structure is suspended from the balloon and the yoke servoed in the North/South meridian plane by error signals from either a magnetometer or star tracker. The detector is commanded to fixed positions in declination and hour angle.

and background is obtained before and after the observation. Then the detector is advanced in hour angle in such a way that a second drift scan may be obtained. This process is continued until as many observations as required have been obtained or until the source is too low in elevation to obtain successful results. Between observations the detector is calibrated by commanding it to a position so that it observes a radioactive source. In order to verify pointing position the sky is photographed with a camera attached to the polar axis. Although the design goal is for a pointing accuracy on the order of 0.1° , about 0.3° rms has been obtained. It is felt that continued refinements of the servo mechanisms and mechanical integrity of the structure will permit attainment of the design goal with this rather simple configuration.

Data are telemetered on an FM/FM/PCM link. Events from the pulse height analyzer are coded on a PCM word which is transmitted, along with data relative to total counting rates, background effects, deadtime, detector mode, etc., on the PCM format. Information required to operate the pointing controls and various other housekeeping functions is transmitted on additional subcarriers. Data are decoded in a standard PCM ground station and spectra are displayed by reading events into the memory core of a laboratory pulse height analyzer. Data are also recorded, along with timing information, on magnetic tapes which are processed through a computerized system after the flight has been performed.

Although the detector and observation system described here represents the present state-of-the-art development at UCSD, most of the observations which are discussed here were performed with relatively simpler systems developed during the evolution of detector, pointing, and communication techniques.

3. The Crab Nebula

The Crab Nebula was the first X-ray source to be positively identified with a known optical or radio object (Bowyer *et al.*, 1964). It was also the first source to be detected via a balloon observation by Clark in 1964 (Clark, 1965). Since then it has been studied extensively from balloons at UCSD. The spectrum obtained from our work (Peterson *et al.*, 1968) together with certain other results at higher (Haymes *et al.*, 1968a) and lower energies (Chodil *et al.*, 1967) are shown in Figure 4. There are also many additional observations, all of which are in general agreement with the spectrum in Figure 4. The data now available on the Crab Nebula form a continuous spectrum defined between 1 and 500 keV, which has a power law shape. Under present thinking, this is indicative of a synchrotron process.

If indeed X-rays are produced by synchrotron radiation in the 10^{-4} G field of the Nebula, the predicted lifetime of the electrons which produces 50 or 100 keV X-rays is only on the order of a few hours. Unless the process which accelerates the electrons to produce these X-rays is rather continuous, one should expect to see time variations in the X-ray spectrum. Therefore, it is germane to observe the Crab Nebula as sensitively and as often as possible in order to search for these variations. Observations at UCSD using essentially the same detector, which avoids systematic effects, have

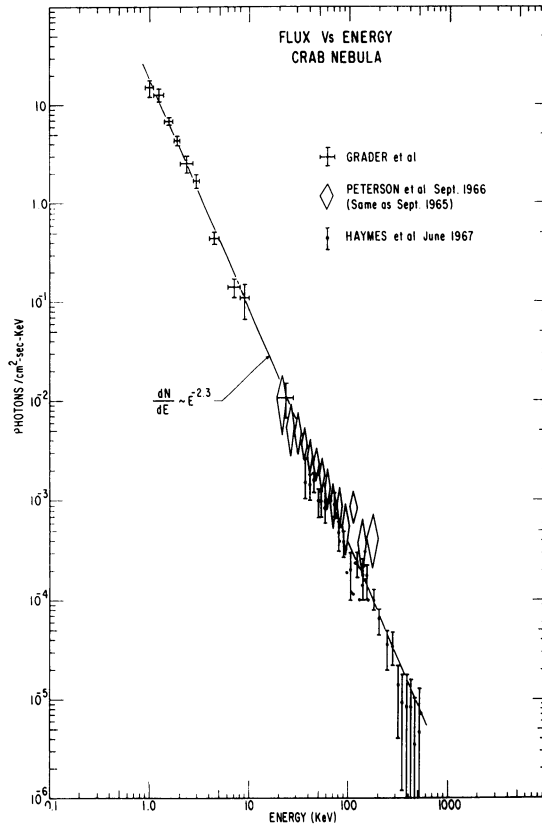


Fig. 4. The spectra of the Crab Nebula determined by a series of rocket and balloon observations over the 1–500 keV range. The data are all consistent with a power law spectrum, suggesting a synchrotron process.

been obtained over the 22-month period from September 1965 through July 1967. On three flights, 22 September 1965, 21 September 1966, and 7 July 1967 (Jacobson, 1968), no significant changes were observed over the 30–100 keV range. At a 95% confidence level, hard X-rays from Crab Nebula must be constant within 3% per year. This small variation presents remarkable constraints upon the accelerator if indeed the synchrotron process is responsible for these X-rays.

In addition to studying the continuous emission from the Crab Nebula, effort has been devoted to search for γ -ray line emission. Such lines have been predicted based upon the production of *r*-process elements in the supernova explosion (Clayton and Craddock, 1965). The model for these predictions is the production of fissionable Cf^{254} , which was advanced to explain the 55-day decay associated with Type I supernovae. If indeed Cf^{254} is produced in the initial explosion, other heavy elements should also have been formed and some of the longer half-life products presently undergoing radioactive decay in the remnant. The activities predicted have been calculated initially by Clayton and Craddock and include lines due to Am^{241} , Cf^{251} , and Cf^{249} .

Jacobson (1968) of UCSD has made an extensive search for these lines using a germanium-lithium drifted cooled detector in an active anticoincidence shield similar to that flown on the OSO-III. These observations were made with a 10 cm² area detector, 5 mm thick, which was flown in a gondola which had a simple alt-azimuth pointing control. The upper limits obtained by Jacobson from his observations in July 1967 are shown in Table I. This table also shows the initial predictions of Clayton

TABLE I
Upper limits on predicted γ -ray lines from the Crab Nebula

<i>r</i> -Process element	Energy (keV)	Predicted flux [Clayton and Craddock (1965)] (cm ² -sec) ⁻¹	Predicted flux (This work) (cm ² -sec) ⁻¹	Previous upper limits [Haymes <i>et al.</i> (1968)]	Upper limits (This work) (cm ² -sec) ⁻¹
Am 241	59.6	5.7×10^{-5}	5.1×10^{-5}	3.9×10^{-3}	1.4×10^{-3}
X-rays	104	—	4.0×10^{-5}	—	1.0×10^{-3}
Cf 251	180	1.9×10^{-5}	7.6×10^{-5}	1.5×10^{-3}	1.1×10^{-3}

and Craddock as well as corrections to the predicted fluxes based upon improved branching ratios. An additional component, that of KX-rays of the heavy elements, has also been added by Jacobson. The predictions are about a factor of 20 below the present upper limits.

These upper limits, however, are based upon the assumption that all of the fission energy of Cf²⁵⁴ is emitted as light and that this is the principle energy source. Any inefficiency will result in a higher γ -ray intensity. Furthermore, these intensities were predicted under the assumption that the distance to the Crab was approximately 1.3 Kpcs. Recent measurements by Trimble (1968) indicate a new distance of 2.02 Kpcs. At this distance the optical extinction is larger, which results in an increase in the expected γ -ray line intensity. At the new distance the upper limits are only a factor of four above the predicted line intensities for an efficiency of unity (Jacobson, 1969). Thus, the upper limits and the predicted fluxes are bracketed within a rather narrow range, and it seems that the efficiency for conversion of fission energy through ionization into light energy must have been at least 25%, and that this efficiency must have maintained during the large expansion of the nebula that occurred immediately following the explosion.

Therefore, based on these results it seems that the Cf²⁵⁴ fission is becoming rather untenable as an explanation for the initial energy source of the Crab Nebula. There are other considerations which involve the dynamics of the expansion, heating, etc. (Sartori and Morrison, 1967), which have also cast doubt upon this idea in recent years. It would seem that only a small increase in sensitivity could absolutely disprove this hypothesis.

The recent discovery of Pulsar NP0532 has, of course, cast an entire new dimension to the study of the Crab Nebula. Since this pulsar has now been observed in the optical range (Cocke *et al.*, 1969) and recently in the rocket X-ray range (Fritz *et al.*, 1969),

the search for pulses in the 20–100 keV spectral range becomes a most important effort. Jacobson (private communication) has reanalyzed the data from his July 1967 flight in order to search for such pulses, and has found an upper limit for pulsed X-ray emission over this range of equal to or less than 15% of the continuous emission. This is not in disagreement with the result reported by Haymes at this meeting (Fishman *et al.*, 1970) of $7 \pm 2\%$ for the pulsed emission over the 40–100 keV range.

4. Scorpius XR-1

The original determination of the spectrum of Scorpius over the 20–50 keV range made by UCSD in June 1965 (Peterson and Jacobson) indicated that the major emission was of an exponential character, suggesting thermal emission from a thin gas at 50×10^6 K. Since then many workers have confirmed this spectrum and have extended it to higher energies. SCO XR-1, the strongest X-ray source in the sky at 3 keV, has now been identified with a 13th magnitude blue optical object which undergoes a number of different time variations (Mook, 1967). These include fast flickering, occasional flare-like events where the optical flux approximately doubles, and slow variations in which the optical flux varies over a period of hours or days by about an optical magnitude. If indeed the X-ray emission from Scorpius is due to a hot gas, as the spectral measurements and other evidence indicate, it would seem that the X-ray emission and the optical emission must be coupled, and the variations should be correlated. Attempts to perform simultaneous observations have been made by the Lawrence Radiation Laboratory from short duration rocket flights, in conjunction with photometric observations by Hiltner (Chodil *et al.*, 1968b). UCSD has also attempted simultaneous observations from balloons in order to observe the higher energy component over an interval of several hours.

These observations were performed May 21/22, 1968, in cooperation with Dr. Hugh Johnson, using the KPNO 84-inch telescope. The optical observations were made with approximately a 10-sec integrating time constant and using three different wavelength filters. One was approximately 20 Å wide centered around $H\beta$, one a wide band filter of 109 Å, also centered at $H\beta$ and therefore included mostly the continuum near $H\beta$; and the third filter was 84 Å wide and included the features associated with $He II$ at 4686 Å. Observations are also made on a comparison star. The filters and reduction procedures have been described previously (Johnson and Golson, 1968).

The 20–40 keV X-ray flux measured during the balloon flight, shown in Figure 5, was observed with the original 48 cm², 8.4° FWHM honeycomb collimated detector. The large increase during the ascent is due to the cosmic-ray transition maximum. Once the balloon reached floating altitude, a rather steady background of both cosmic and atmospheric X-rays was obtained, after which three drift scan transits of the object through the detector aperture were made. To obtain the flux due to Scorpius, after subtracting the background, it is necessary to correct for the position of the source within the aperture using the orientation information and the detailed aperture

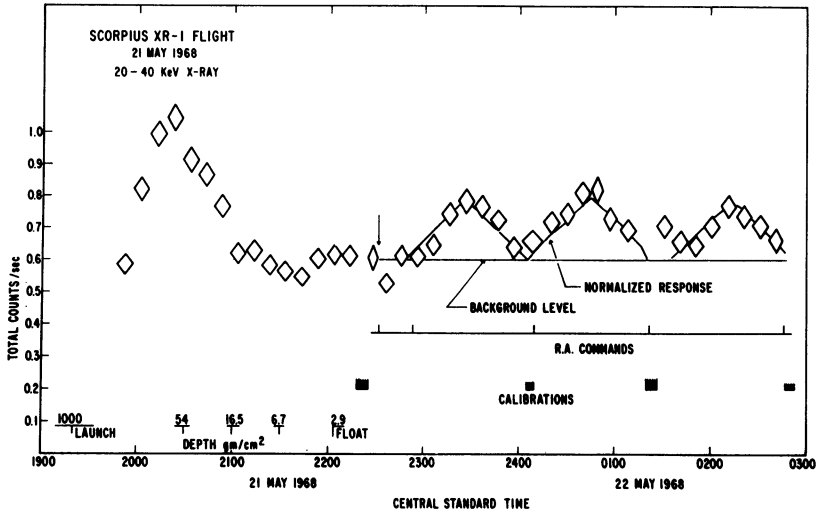


Fig. 5. Counting rates are a function of time during the SCO XR-1 observations of May 21/22, 1968. Background was obtained before and after the three transits of the source.

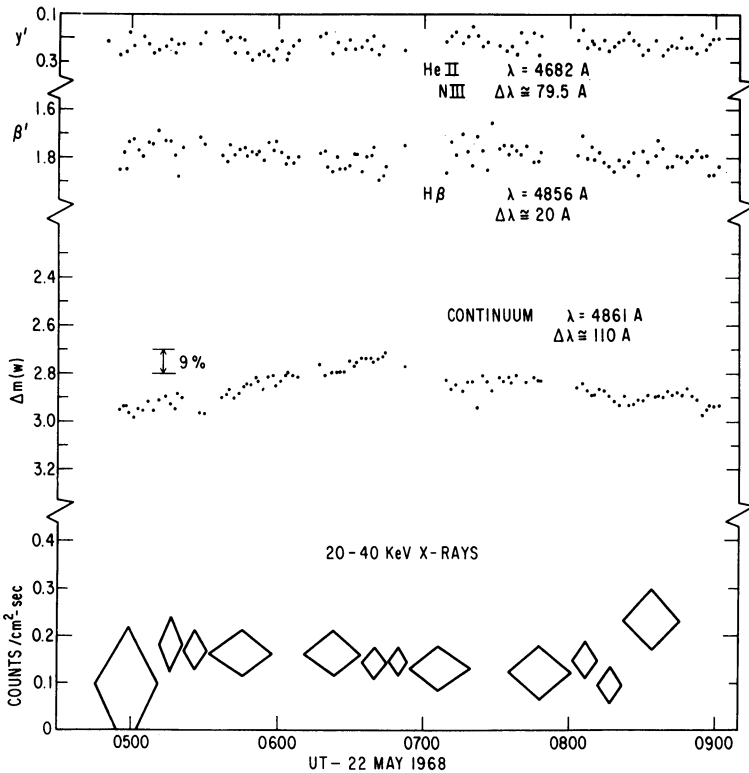


Fig. 6. Corrected counting rates due to X-rays from Scorpius as a function of time compared with simultaneous optical observations. Although the optical intensity varied approximately 25%, statistically significant variations in the total X-ray flux were apparently not observed.

response. The results of carrying out these corrections are indicated in Figure 6 along with the results obtained by Johnson over the various wavelength ranges. Clearly, no variations were obtained from the comparison source (y') or the narrow band centered upon $H\beta$ (β'). The wide band, however, showed a slow increase followed by a decrease during the three-hour observing period. Statistically significant variations of the total X-ray flux over the 20–40 keV energy range were not observed.

Significant changes were, however, observed in the spectrum during each of the three transits. In order to relate these changes to a physically meaningful variable, a thermal emitting source was assumed. The expected measured spectrum was then computed, taking account of atmospheric absorption, detector angular response and efficiency, and resolution spreading. These spectra were then fitted to the measured data using a least square method with temperature as a parameter.

The results of this process are shown in Figure 7, where the best fit incident spectrum,

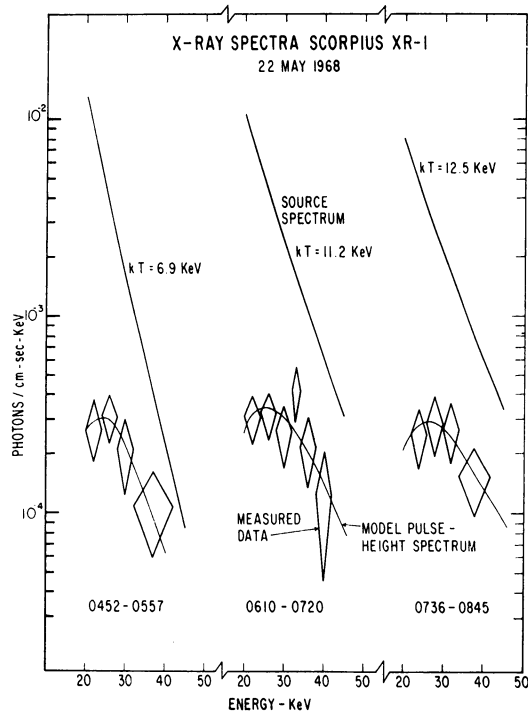


Fig. 7. Spectra of Scorpius determined during each of the three transits. Using a thermal bremsstrahlung spectrum as an input, the expected spectrum at the detector has been computed and is least-square fitted to the measured data using temperature as a parameter.

the model pulse height spectrum at the detector, and the data are all shown for each of the three intervals. The calculated standard deviation of temperature as a parameter is ± 3 keV; a chi-squared test, however, permits the temperature to have remained constant. The higher best-fit temperatures are associated with increased optical emission

as observed by LRL (Chodil *et al.*, 1968b). The variation of total flux at a given energy is a complex function of the change of temperature and emission measure. It is felt, however, that the lack of observed flux change within 20% is not inconsistent with the LRL interpretation based on a thermal model sufficiently compact to be self-absorbing in the optical range.

Observations of time variations of Scorpius have also been obtained from the OSO-III satellite, whose data reduction and analysis have been accomplished by H. S. Hudson and D. A. Schwartz. The 10 cm² OSO-III detector, which is shown in Figure 8,

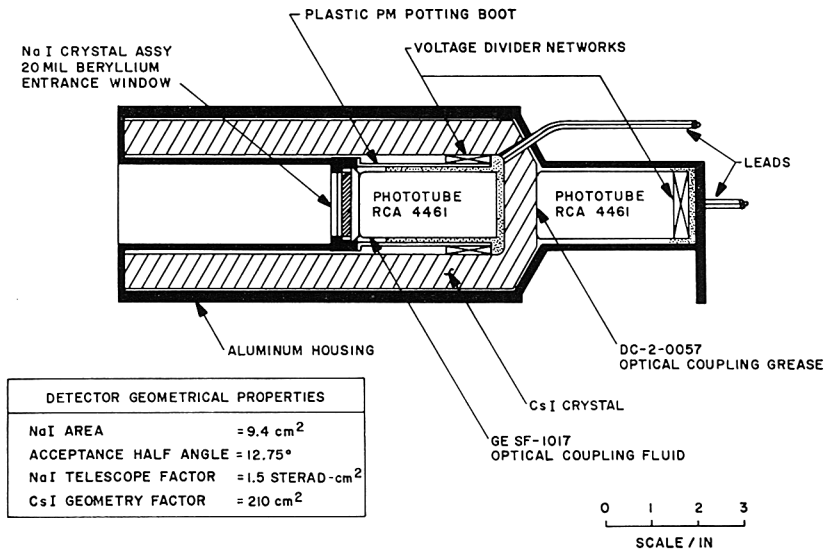


Fig. 8. This detector, located on the rotating wheel section of the OSO-III satellite measures solar, cosmic and background X-rays over the 7.7–200 keV range.

is the earliest version of the anticoincidence shielded detectors developed at UCSD. This detector is mounted looking radially outward in the rotating wheel section of the OSO satellite, and therefore scans across the sky, the sun, and usually the earth with every two-second rotation period. Because the OSO wheel plane is constrained to lie in the earth-sun line, the scan plane precesses at about a degree per day and, as shown in Figure 9, slowly moves across the sky, drifting mostly in hour angle. A point source near the equatorial plane, therefore, slowly drifts across the aperture over a period of about a month.

The X-ray spectrum between 7.7 and 200 keV is obtained in six logarithmically spaced channels with approximately 1.7 energy ratio. Data are obtained in a number of different satellite-programmed modes. One of these accumulates X-rays from the solar direction and reads out every 15 sec; another reads a direction signature for each non-solar event and sequences through the six channels every 12 min. The third, or background mode, which is relevant to the results described here, consists of simply

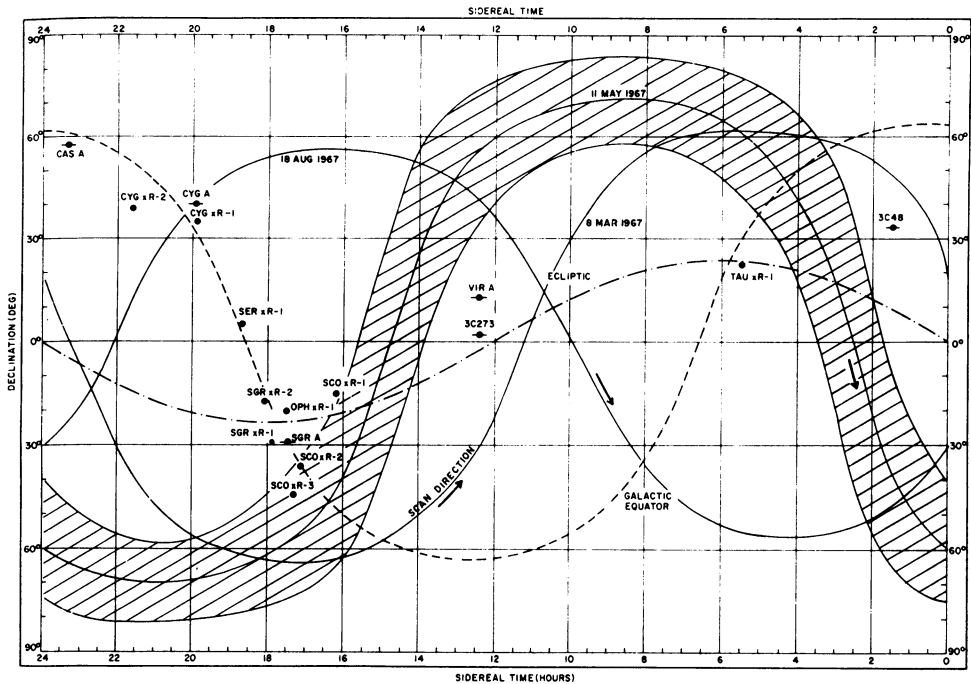


Fig. 9. The area on the celestial sphere scanned by the OSO-III detector during each two-second wheel rotation. Since the scanned plane precesses approximately one degree per day in r.a., a source such as Scorpius slowly drifts through the aperture.

reading out the total counts accumulated during 1.96 sec in each channel every 15 sec during nighttime satellite operation. These events include a mixture of background, diffuse and point cosmic sources, and earth albedo. Scorpius XR-1 dominates the counting rate in this mode even though the source itself is within the aperture of the detector only 7% of each 2-sec scan. This mode was intended to obtain background information necessary to correct data from the solar and the sky modes; the effect of a strong point source such as Scorpius was not anticipated.

Figure 10 shows the counting rates obtained in the lowest channel during May and June of 1967 when the source made its first drift across the scan plane of the satellite. Data are selected to eliminate trapped radiation effects and averaged so that each point has a 10% or smaller statistical error. Background obtained before and after the scan plane intercepts Scorpius is at a level of 1.3 counts/sec.

Also shown is the predicted response based on the assumption that the background is 1.3 counts/sec and that the flux of Scorpius is that indicated by our earlier balloon observation (Peterson and Jacobson, 1966). Calculations include the model spectrum of Scorpius

$$F(E) dE = 110 e^{-(E/4.3)} \text{ keV/cm}^2\text{-sec-keV,}$$

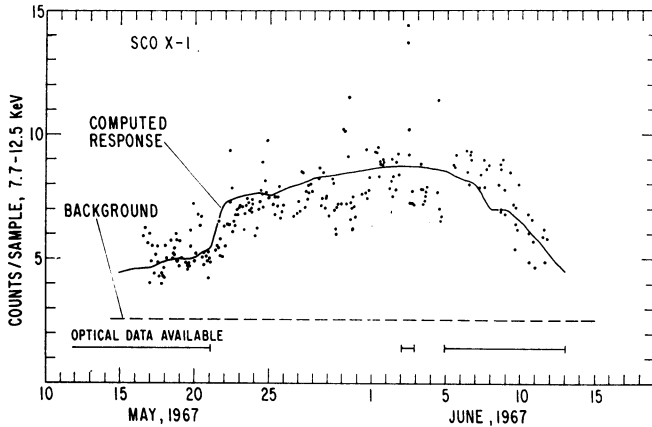


Fig. 10. The total counting rate observed on the OSO-III in the lowest channel during May-June 1967, as Scorpius was drifting through the detector aperture. This strong source so dominates the total counting rate that it is significantly above the background level, as determined before and after the source entered the aperture.

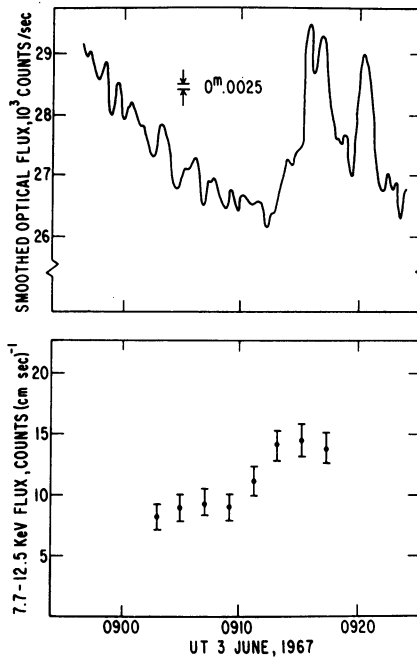


Fig. 11. Simultaneous X-ray and optical observations of the Scorpius flare 0910 on 3 June 1967. The optical observations were fortuitously obtained at the Mt. Wilson telescope.

the instrument response and efficiency and the detailed aspect solution for the satellite. The observed data follows closely the predicted rates, which indicates that we are observing Scorpius, and that the flux is, on the average, close to that measured previously. The fact that some of the data depart from the predicted value more than

the statistics would allow suggests that there are X-ray variations in Scorpius.

Fortuitously, optical observations were also being made during this period, as indicated in Figure 10. These have been obtained from two primary sources: B magnitude photometry obtained on the 36" Cerro Tololo telescope and some high time resolution broad band photometric observations on the Mt. Wilson/Palomar telescopes. Correlations of the optical and X-ray observations for slow variations have not yet been completed, since these data are in a most preliminary form.

One striking result, however, is the confirmation of the observation by MIT (Lewin *et al.*, 1968a) of X-ray flares on Scorpius and their correlation with the related optical phenomena. The optical observations were made by Westphal *et al.* (1968) on the 100-inch telescope on the night of 3 June 1967. Figure 11 shows the Scorpius flare of 0910 on the 3 June observation by the satellite OSO-III and also the correlated optical data. Over a 5-min period the X-ray flux nearly doubled, while the optical flux increased about 25%. Although the accuracy of the time comparison is only about two minutes, these results indicate that X-ray flares and optical flares on Scorpius are

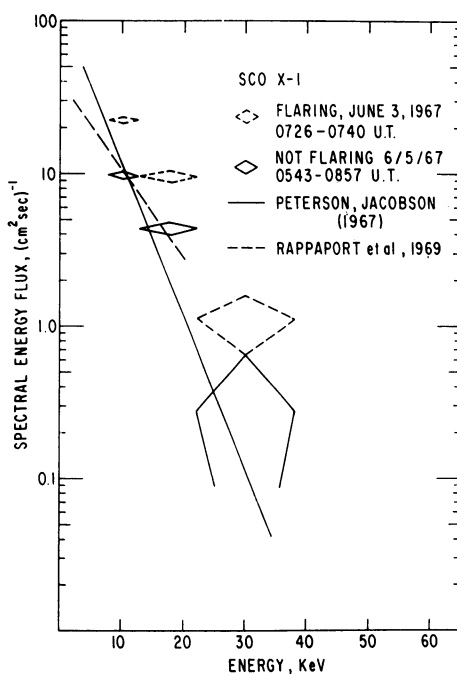


Fig. 12. The Scorpius flare spectrum as determined during another flare on 3 June. According to these data, the spectral shape of the flare is very similar to that of quiescent Scorpius.

indeed related phenomena. Another flare was observed on the same night at 0725. Figure 12 shows the X-ray spectrum from this flare. The flare spectrum as deduced from this observation indicates a uniform increase in all channels over the pre-flare flux. This is in disagreement with the observation of Clark in which he inferred that

the flare spectrum was softer than that of the quiescent object. Although additional observations will be required to settle this and other questions, this work has indicated for the first time that X-ray and optical flares do indeed occur simultaneously on Scorpius XR-1.

The combination of optical, radio, rocket and balloon X-ray observations have now indicated a model for Scorpius. Figure 13 shows the fluxes which have been observed in all spectral ranges. These observations and their time variations imply a model for

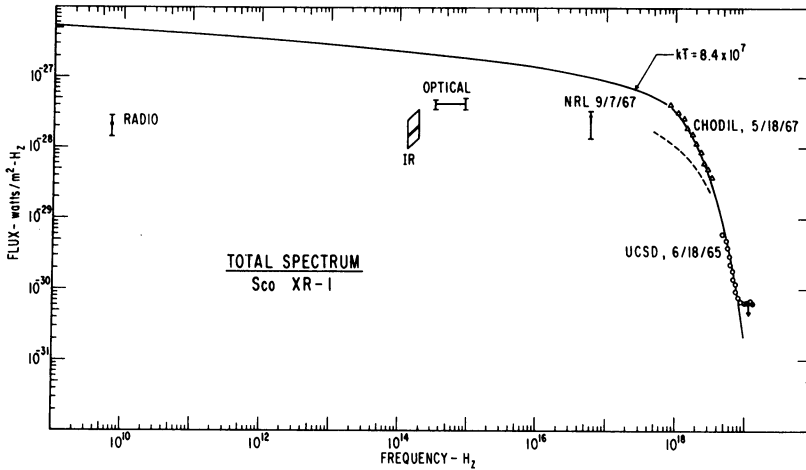


Fig. 13. A summary of radio, optical and X-ray observations of SCO XR-1 compared with the thermal bremsstrahlung expected from an optically thin object uniformly at 84×10^6 K. The data demand a more complex model.

Scorpius in which the object consists of a hot gas, on the order of 50×10^6 degrees, which is rather compact and becomes optically thick in the infrared range, and therefore follows the Rayleigh-Jeans law in emission (Neugebauer *et al.*, 1968). The source must have a diameter of approximately 10^8 cm and a density of $10^{16}/\text{cm}^3$ based upon a distance of 0.17 kpc. (Gatewood and Sofia, 1968). The 'high energy tail' of hard X-rays may be due to an additional component of electrons, and the object must be associated with a cooler region to account for the atomic emission lines. The radio observations are not consistent with a compact thermal source. The radio data and the higher energy X-rays have been related in a model by Riegler and Ramaty (1969), in which an additional region of 10^{12} cm radius and rather lower density which contains a magnetic field is postulated. The electrons which produce the radio emission by synchrotron radiation are responsible for the higher energy X-rays by bremsstrahlung.

5. Other Sources

In addition to the Crab Nebula and Scorpius, which have been studied extensively, a number of other sources have been observed from the OSO-III satellite and from

balloons. Because of the design of the detectors used at UCSD, broad sky surveys from balloons are not attempted and observations are generally made on X-ray sources identified from rocket observations. Sky surveys at high sensitivity are best accomplished from satellites.

The spectrum of the X-ray source which has been associated with the object M-87 (Bradt *et al.*, 1967) is of considerable interest since it is the only known extra-galactic X-ray source. This very weak X-ray source, $\frac{1}{30}$ of the Crab Nebula at 3 keV, may be observed at balloon altitude with sufficiently sensitive technique if the spectrum is not too soft. A series of upper limits on this object obtained at UCSD are shown in Figure 14. M-87 is below the level of detectability of the OSO-III satellite; therefore,

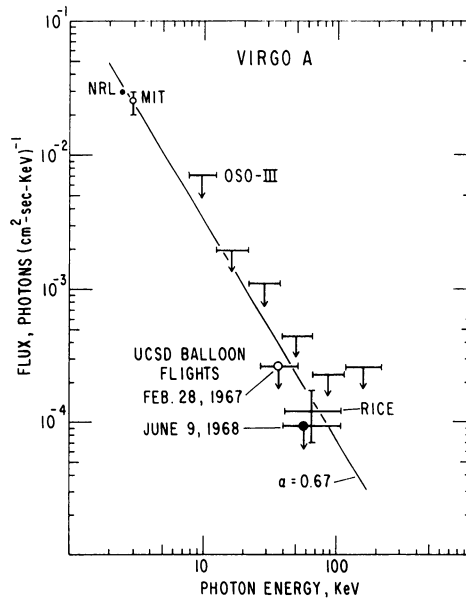


Fig. 14. A summary of the upper limits on M-87 obtained from the OSO-III satellite and from the series of balloon flights at UCSD. Also shown are the fluxes measured at rocket energies and the reported flux at 40 keV by Rice University.

only upper limits are available. Two attempts have been made to detect this object from balloons, one during February 1967, and again during June of 1968. Although neither of these flights was sufficiently successful so that the ultimate sensitivity of the observation could be realized, significant upper limits have nevertheless been obtained, as shown in Figure 14. These upper limits, which are at a 3σ confidence level, seem to be significantly below the reported flux at 40 keV due to Haymes at Rice University (Haymes *et al.*, 1968c). We therefore question the validity of the Rice observation.

A series of observations have also been obtained of the Cygnus region. Cygnus X-1, which at the higher energies seems to have a power law spectrum of similar intensity and slope to the Crab Nebula, was originally observed by UCSD in September 1966

(Peterson *et al.*, 1968) and has been reobserved by Jacobson and Laros in 1968 (private communication). A summary of selected results is shown in Figure 15, compared with the UCSD observations. Time variations have been reported for this source and the large scatter of the rocket data indicates that this is indeed the case. The UCSD observations do not presently extend to high enough energy to verify the

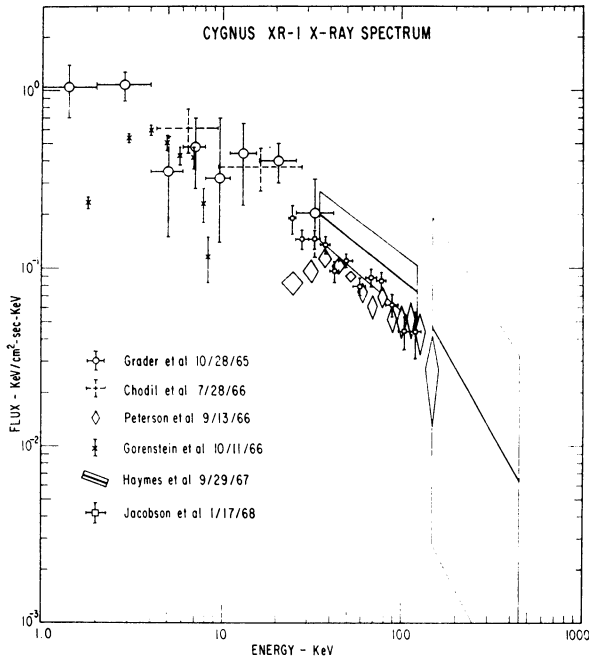


Fig. 15. The spectrum of Cygnus XR-1 determined from a series of balloon and rocket observations. Although there seems clear evidence of time variations at the lower energies, the two UCSD observations are consistent with a simple power law spectra over the 30–100 keV range.

break in the spectrum at about 150 keV reported by Haymes (Haymes *et al.*, 1968b).

The spectrum of the weak source Cygnus XR-3 has also been determined on a balloon flight on 22 May, 1968. All of the data on this source are shown in Figure 16. Although this object appears to have a thermal spectrum at lower energies (Giacconi *et al.*, 1967), an additional hard component is indicated above about 20 keV. It may be that all sources which appear to be thermal-like over the rocket range have additional hard components associated with them, such as has already been indicated for Scorpius.

The OSO-III has made observations of certain sources in the southern sky, some of which will be presented here in a preliminary form. Figure 17 shows the source Norma XR-2 at 15 hr, 32 min r.a., -57° dec. This source was first identified in a rocket survey (Friedman *et al.*, 1967), observed from a balloon by Lewin and Clark (Lewin *et al.*, 1968b) and was previously identified erroneously with Lupus XR-1 in a UCSD preprint (Schwartz *et al.*, 1968). No significant change was observed in this

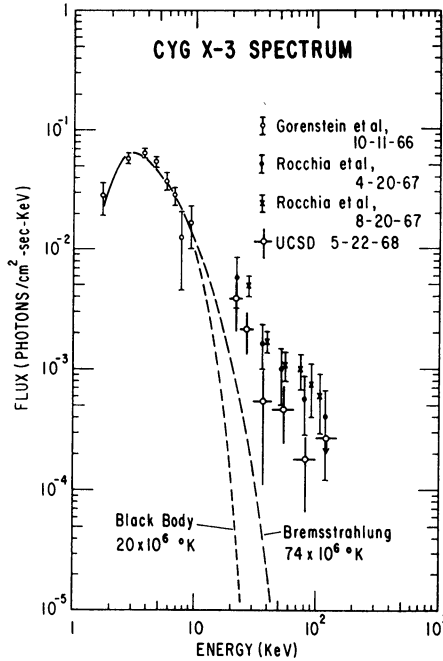


Fig. 16. The Cygnus X-3 spectrum as determined from several observations. Although this source is consistent with thermal bremsstrahlung at lower energies, there is apparently, like Scorpius, an additional component at the higher energies.

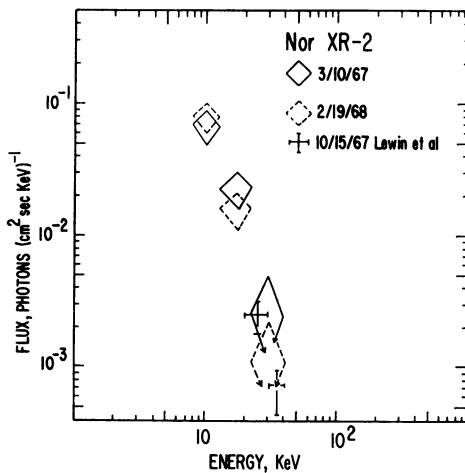


Fig. 17. Spectrum of Norma XR-2 determined on two different occasions by the OSO-III satellite, compared with the balloon observation of Lewin and Clark. Over nearly a year there is no evidence of time variation.

source between 10 March 1967 and 19 February 1968. The spectrum agrees with the observation on 15 October 1967 by Lewin and Clark. Norma XR-2 apparently is not a variable source within about 20% over a one-year period.

The variable X-ray source Centaurus XR-2 has also been observed by the OSO-III. Originally discovered by rockets during May and June 1967, it suddenly appeared and subsequently decayed with a 30-day time constant (Chodil *et al.*, 1968a). It is located

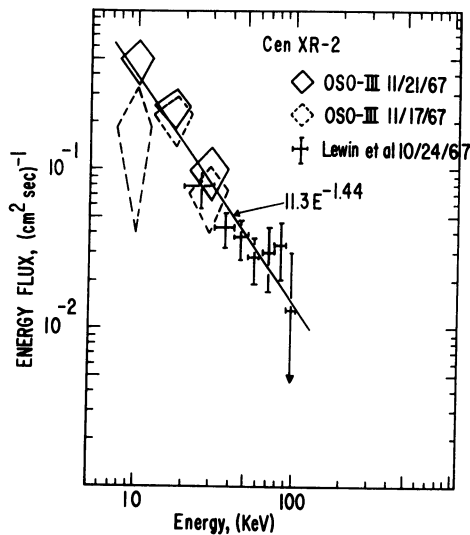


Fig. 18. The variable source Centaurus XR-2 measured during October and November 1967 by the OSO-III compared with the balloon measurement of Lewin and Clark.

at 196.5° r.a., -64° dec and has been tentatively identified with the Nova WX Centaurus (Eggen *et al.*, 1968). Lewin and Clark observed this source 24 October 1967 to have a hard component, although rocket observations indicated that the source was no longer observable (Chodil *et al.*, 1968a). The OSO-III observations were during November 1967, and by January and February of 1968 the source had decreased below the threshold of detectability over the 10–100 keV range. The spectral data obtained in October and November of 1967 are summarized in Figure 18.

Conclusion

In this brief presentation we have tried to review some of the significant results which have been obtained by the UCSD X-ray and Gamma-ray Astronomy Group on individual point sources during the past several years. Balloon observations of the sources in the Northern Hemisphere are continuing, and the reduction of the OSO-III satellite will be completed very shortly. From these data it is hoped to obtain information on the spectra and time variations of 10 or 15 of the strongest sources in the sky. These results will be published in the literature. In addition this experiment will

provide data on the isotropy and spectrum of the cosmic background component (Hudson *et al.*, 1969). This component has also been studied extensively at UCSD using the ERS-18 satellite where the spectrum has been extended to approximately 6 MeV (Vette *et al.*, 1970).

Acknowledgements

This research was supported under NASA Grant NSG-318 and Contract NAS5-3177 with the Goddard Space Flight Center. In addition to those directly mentioned, the author acknowledges the work of many other students, staff and colleagues who have contributed to these experiments.

References

- Bowyer, S., Byram, E. T., Chubb, T. A., and Friedman, H.: 1964, 'Lunar Occultation of X-Ray Emission from the Crab Nebula', *Science* **146**, 912.
- Bradt, H., Mayer, W., Naranan, S., Rappaport, S., and Spada, G.: 1967, 'Evidence for X-Radiation from the Radio Galaxy M-87', *Astrophys. J. Letters* **150**, L199.
- Chodil, G., Mark, Hans, Rodrigues, R., Seward, F. D., and Swift, C. D.: 1967, 'X-Ray Intensities and Spectra from Several Cosmic Sources', *Astrophys. J.* **150**, 57.
- Chodil, G., Mark, Hans, Rodrigues, R., and Swift, C. D.: 1968a, 'Nova-Like Behavior of the X-Ray Source Centaurus XR-2', *Astrophys. J. Letters* **152**, L45.
- Chodil, G., Mark, Hans, Rodrigues, R., Seward, F. D., Swift, C. D., Turiel, Isaac, Hiltner, W. A., Wallerstein, George, and Mannery, E. J.: 1968b, 'Simultaneous Observations of the Optical and X-Ray Spectra of SCO XR-1', *Astrophys. J.* **154**, 645.
- Clark, George W.: 1965, 'Balloon Observation of the X-Ray Spectrum of the Crab Nebula above 15 keV', *Phys. Rev. Letters* **14**, 91.
- Clayton, D. D. and Craddock, W. L.: 1965, 'Radioactivity in Supernova Remnants', *Astrophys. J.* **142**, 189.
- Cocke, W. J., Disney, M. J., and Taylor, D. J.: 1969, *Nature* **221**, 525.
- Eggen, O. J., Freeman, Kenneth C., and Sandage, Allan: 1968, 'On the Optical Identification of the X-Ray Source CEN XR-2 as WX CEN', *Astrophys. J. Letters* **154**, L27.
- Fishman, G. J., Harnden, F. R., and Haymes, R. C.: 1970, this volume p. 116.
- Friedman, H., Byram E. T., and Chubb, T. A.: 1967, 'Distribution and Variability of Cosmic X-Ray Sources', *Science* **156**, 3773, 374.
- Fritz, G., Henry, R. C., Meekins, J. F., Chubb, T. A., and Friedman, H.: 1969, 'X-Ray Pulsar in the Crab Nebula', *Science* **164**, 3880, 709.
- Frost, K. J., Rothe, E. D., and Peterson, Laurence E.: 1966, 'A Search for the Quiet-Time Solar Gamma-Rays from Balloon Altitudes', *J. Geophys. Res.* **71**, 17, 4079.
- Gateway, George and Sofia, Sabatino: 1968, 'Physical Characteristics of SCO X-1', *Astrophys. J. Letters* **154**, L69.
- Giacconi, R., Gorenstein, P., Gursky, H., and Waters, J. R.: 1967, 'An X-Ray Survey of the Cygnus Region', *Astrophys. J. Letters* **148**, L119.
- Haymes, R. C., Ellis, D. V., Fishman, G. J., Kurfess, J. D., and Tucker, W. H.: 1968a, 'Observation of Gamma Radiation from the Crab Nebula', *Astrophys. J. Letters* **151**, L9.
- Haymes, R. C., Ellis, D. V., Fishman, G. J., Glenn, S. W., and Kurfess, J. D.: 1968b, 'Detection of Gamma Radiation from the Cygnus Region', *Astrophys. J. Letters* **151**, L125.
- Haymes, R. C., Ellis, D. V., Fishman, G. J., Glenn, S. W., and Kurfess, J. D.: 1968c, 'Detection of Hard X-Radiation from Virgo', *Astrophys. J. Letters* **151**, L131.
- Hicks, D. B., Reid, L. Jr., and Peterson, L. E.: 1965, 'X-Ray Telescope for an Orbiting Solar Observatory', *IEEE Trans. Nucl. Sci.* **NS-12**, 54.
- Hudson, H. S., Peterson, L. E., and Schwartz, D. A.: 1969, 'Solar and Cosmic X-Rays above 7.7 keV', *Solar Phys.* **6**, 205.

- Jacobson, A. S.: 1968, A Search for Gamma-Ray Line Emissions from the Crab Nebula, Thesis.
- Jacobson, A. S.: 1969, The Gamma-Ray Line Spectrum of the Crab Nebula (UCSD Preprint).
- Jerde, R. L., Peterson, L. E., and Stein, W.: 1967, 'Effects of High Energy Radiations on Noise Pulses from Photomultiplier Tubes', *Rev. Sci. Instr.* **38**, 1387.
- Johnson, H. M. and Golson, J. C.: 1968, 'Narrow-Band and UVB Photometry of GX3-1 and Two Wolf-Rayet Stars', *Astrophys. J. Letters* **154**, L77.
- Lewin, W. H. G., Clark, G. W., and Smith, W. B.: 1968a, 'Observation of an X-Ray Flare from SCO X-1', *Astrophys. J.* **152**, L55.
- Lewin, W. H. G., Clark, G. W., and Smith, W. B.: 1968b, 'Observation of CEN XR-2 and Other High-Energy X-Ray Sources in the Southern Sky', *Astrophys. J. Letters* **152**, L49.
- Mook, Delo E.: 1967, 'UBV Photometry of SCO XR-1', *Astrophys. J.* **150**, L25.
- Neugebauer, G., Oke, J. B., Becklin, E., and Garmire, G.: 1969, 'A Study of Visual and Infrared Observations of SCO XR-1', *Astrophys. J.* **155**, 1.
- Overbeck, James W. and Tananbaum, Harvey D.: 1968, 'Time Variations in Scorpius X-1 and Cygnus XR-1', *Astrophys. J.* **153**, 899.
- Peterson, L. E.: 1966, 'Upper Limits of the Cosmic Gamma-Ray Flux from OSO-I', *Space Research*, Vol. VI, p. 53.
- Peterson, L. E. and Jacobson, A. S.: 1966, 'The Spectrum of SCO XR-1 to 50 keV', *Astrophys. J.* **145**, 962.
- Peterson, L. E., Jerde, R. L., and Jacobson, A. S.: 1967, 'Balloon X-Ray Astronomy', *AIAA J.* **5**, 1921.
- Peterson, L. E., Jacobson, A. S., Pelling, R. M., and Schwartz, D. A.: 1968, 'Observations of Cosmic X-Ray Sources in the 10–250 keV Range (Presented at 10th International Cosmic Ray Conference, Calgary, Canada, June 1967) *Can. J. Phys.* **46**, S437.
- Riegler, G. and Ramaty, R.: 1969, 'Physical Properties of the Radio-Emitting Region of SCO X-1 (GSFC X-611-69-123)'; Preprint March.
- Sartori, L. and Morrison, P.: 1967, 'Thermal X-Rays from Non-Thermal Radio Sources', *Astrophys. J.* **150**, 385.
- Schwartz, D. A., Hudson, H. S., and Peterson, L. E.: 1968, 'Satellite Observation of the X-Ray Source in Lupus', Preprint January 1969.
- Trimble, Virginia: 1968, 'Motions and Structure of the Filamentary Envelope of the Crab Nebula', *Astron. J.* **73**, 535.
- Vette, J. I., Matteson, J. L., Gruber, D., and Peterson, L. E.: 1970, this volume p. 355.
- Westphal, J. A., Sandage, Allan, and Kristian, Jerome: 1968, 'Rapid Changes in the Optical Intensity and Radial Velocities of the X-Ray Source SCO X-1', *Astrophys. J.* **154**, 139.